

Original Article

Cite this article: Landaeta MF, Nowajewski V, Paredes LD, Bustos CA (2019). Early life history traits of the blenny *Auchenionchus crinitus* (Teleostei: Labrisomidae) off northern Chile. *Journal of the Marine Biological Association of the United Kingdom* **99**, 969–974. <https://doi.org/10.1017/S0025315418000619>

Received: 5 January 2018

Revised: 9 July 2018

Accepted: 23 July 2018

First published online: 28 September 2018

Key words:

Antofagasta; ichthyoplankton; nearshore; sagittae

Author for correspondence:

Mauricio F. Landaeta, E-mail: mauricio.landaeta@uv.cl

Early life history traits of the blenny *Auchenionchus crinitus* (Teleostei: Labrisomidae) off northern Chile

Mauricio F. Landaeta^{1,2}, Valentina Nowajewski¹, Lissette D. Paredes³
and Claudia A. Bustos¹

¹Laboratorio de Ictioplancton (LABITI), Escuela de Biología Marina, Facultad de Ciencias del Mar y de Recursos Naturales, Universidad de Valparaíso, Viña del Mar, Chile; ²Centro de Observación Marino para Estudios de Riesgo Ambiental (COSTA-R), Universidad de Valparaíso, Viña del Mar, Chile and ³Instituto de Ciencias Naturales Alexander von Humboldt, Universidad de Antofagasta, Antofagasta, Chile

Abstract

The early life history traits of the labrisomid blenny *Auchenionchus crinitus* (Jenyns, 1842) from subtidal rocky reefs were studied, based on microstructure analysis of sagittae of their pelagic larvae (4.01 mm NL –12.50 mm SL). Ichthyoplankton was collected in shallow (<20 m) nearshore waters off Isla Santa María, Antofagasta, northern Chile every 15 days during austral autumn–winter 2014 (five sampling days). During late May and early June, larval abundance was low (median \pm MAD, 39.06 \pm 5.08 ind. 100 m⁻³), increasing significantly during mid-June to early August (110.98 \pm 47.66 ind. 100 m⁻³). Using 354 sagittae, the back-calculated hatch dates indicated the occurrence of three hatching events, two in autumn and one in winter. Hatching occurred mainly during the illuminated phases of the lunar cycle. All three batches had similar estimated larval sizes at hatch (3.2–3.7 mm SL), as well as similar growth rates (0.19–0.22 mm day⁻¹) during the first 30 days of life. During the study period, shallow waters were well mixed, with seawater temperature of 14.73 \pm 0.58°C and salinity of 34.84 \pm 0.04. This is the first estimation of early life history traits of this cryptobenthic species from rocky reefs of Chile.

Introduction

Cryptobenthic fishes have been defined as adult fishes of typically <5 cm that are visually and/or behaviourally cryptic, and maintain a close association with the benthos (Depczynski & Bellwood, 2003). Nonetheless, there are exceptions, with some species (e.g. the giant goby *Gobius cobitis*) reaching up to 30 cm (Gibson, 1970). Except for some viviparous benthic species (such as the eelpout *Zoarces viviparus*), most of them have a bipartite life cycle, with a pelagic larval phase that ends at reef settlement (Leis, 1991), and benthic juvenile and adults. Because of the restricted movement of the latter between reefs, species rely on their pelagic larval duration to disperse and maintain biogeographic ranges as well as connectivity between populations (Riginos & Victor, 2001; Kohn & Clements, 2011).

By revealing early life history traits it is possible to understand pre-settlement processes (Bergenius *et al.*, 2002; Plaza *et al.*, 2013). A powerful tool to reveal early life traits of fishes is the analysis of otolith microstructure (Panella, 1971; Campana & Neilson, 1985). These structures have identifiable banding patterns or rings of daily periodicity that reflect the punctuated nature of growth (Chambers & Miller, 1995), which has been validated in several cryptobenthic fish species (Mansur *et al.*, 2013; Carvalho *et al.*, 2015). By applying otolith microstructure analysis in larval stages of fish it is possible to estimate population and individual growth rates, individual size at time to hatch, yolk sac resorption and onset of exogenous feeding, mortality rates, or to separate larvae which have grown under different environmental conditions or under different moon phases (Robertson *et al.*, 1990; Stenevik *et al.*, 1996; Fontes *et al.*, 2011; Landaeta *et al.*, 2012; Contreras *et al.*, 2017; La Mesa *et al.*, 2017).

One large (up to 18 cm length) cryptobenthic fish typical of shallow waters of north and central Chile is the labrisomid blenny, *Auchenionchus crinitus* (Jenyns, 1842). This subtidal species is distributed from Pucusana, Perú (12°28'S 76°48'W) to Viña del Mar, Chile (33°01'S 71°33'W), and is sympatric with two other species of the genus *Auchenionchus*: *A. variolosus* and *A. microcirrhis* (Stephens & Springer, 1973; Sáez & Pequeño, 2009). Adult labrisomids are carnivorous, preying on crabs, shrimps, isopods and amphipods (Muñoz & Ojeda, 1997), while larvae of *A. variolosus* feed mostly on eggs and nauplii of calanoid copepods (Vera-Duarte & Landaeta, 2016). Daily deposition of microincrements in the sagittae otolith has been validated for *A. crinitus* (Mansur *et al.*, 2013). Nonetheless, there is a lack of information about the early life traits of *A. crinitus*. Therefore, the goal of this study was to analyse the early life history of this labrisomid blenny, during autumn–winter conditions, by using otolith microstructure analysis.



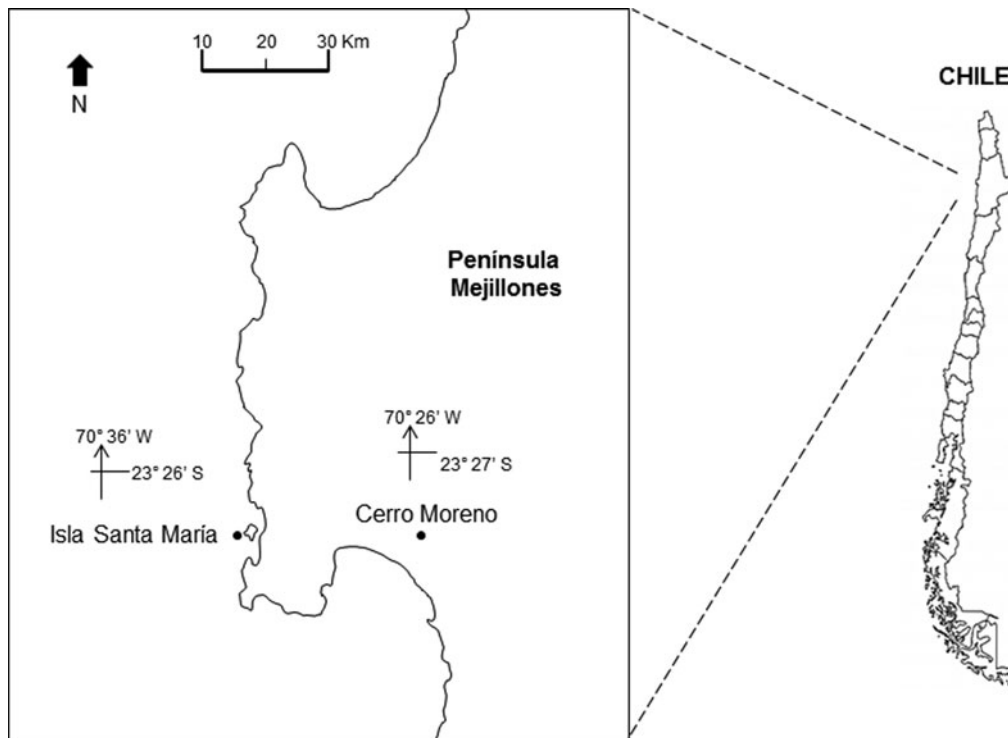


Fig. 1. Location of the study site, Isla Santa María (ISM), Mejillones Peninsula, Antofagasta, northern Chile. The location of the meteorological station, at Cerro Moreno airport, is also indicated.

Table 1. Sampling periods, standardized abundance (ind. 100 m^{-3}) and size structure (NL or SL, mm) of larval labrisomid *Auchenionchus crinitus* from northern Chile during austral autumn–winter 2014

Sampling date	Abundance Median	Abundance MAD	N	Size range	Size median	Size MAD	Skewness	SE skewness	Kurtosis	SE kurtosis
27 May 2014	79.9	24.11	139	4.03–8.47	5.68	0.62	0.28	0.21	−1.2	0.41
15 June 2014	15.99	3.21	83	4.01–7.59	4.92	0.32	1.52	0.26	3.29	0.52
30 June 2014	107.2	58.53	98	4.30–10.0	6.97	0.88	0.27	0.24	1.74	0.48
14 July 2014	72.89	35.54	72	4.36–9.61	6.63	1.02	0.31	0.28	−0.41	0.56
1 August 2014	133.24	74.2	94	6.65–12.50	8.27	0.55	0.62	0.25	2.6	0.49

MAD, median absolute deviation; SE, standard error.

Materials and methods

Study area

The study area is located off northern Chile (Humboldt Current System), at Isla Santa María (ISM) ($23^{\circ}26'S$ $70^{\circ}36'W$) in Mejillones Peninsula (Figure 1). The location is a sheltered area, with artisanal fishing, spear fishing and kelp harvesting. It is characterized by rocky bottom, barren ground and kelp forests of *Lessonia trabeculata* and *Macrocystis integrifolia*. The bathymetry does not exceed 18 m (Uribe *et al.*, 2015).

Fieldwork

The daily prevailing wind was available from a Meteorological Station at Cerro Moreno Airport ($23^{\circ}27'S$ $70^{\circ}26'W$; Figure 1) supervised by the Dirección Meteorológica de Chile. The Ekman transport was estimated to assess the effect of winds on the offshore displacement of surface coastal waters. The equation $M_E = -\tau/f$ was used, where M_E is the Ekman transport ($1000\text{ kg m}^{-1}\text{ s}^{-1}$), f is the Coriolis parameter and $-\tau$ is the along-shore

wind stress at the surface of the water (Pond & Pickard, 1983). Tau (τ) was estimated using the equation: $\tau = \rho_a \times C_d \times W$; where ρ_a is the air density (1.2 kg m^{-3}), C_d is the drag coefficient (0.0014) and W is the along-shore wind speed (m s^{-1}).

Every 15 days between May (austral-autumn) and August (austral-winter) 2014, five dates (S1–S5) were sampled off ISM (Table 1). Temperature and salinity of the water column were obtained with a CTD (Seabird SBE-19 plus) at the beginning and end of every sampling day from surface to 15 m depth. Ichthyoplankton samples were collected using a Bongo net (60 cm mouth diameter; 300 μm mesh size), equipped with one TKS flow meter (The Tsurumi-Seiki Co., Ltd; Tsurumi-ku, Yokohama, Japan) to quantify the filtered water. The plankton was collected parallel to the coastline, at 1–2 knots during 10–15 min from a depth of 10–18 m to surface (double-oblique tow) during the morning, on board an artisanal boat. Every sampling date, eight collections were made. The samples were fixed with 5% formalin buffered with sodium borate ($N = 40$). After 24 h, formalin-fixed samples were preserved in 96% ethanol to avoid negative effects on otolith microstructure of fish larvae.

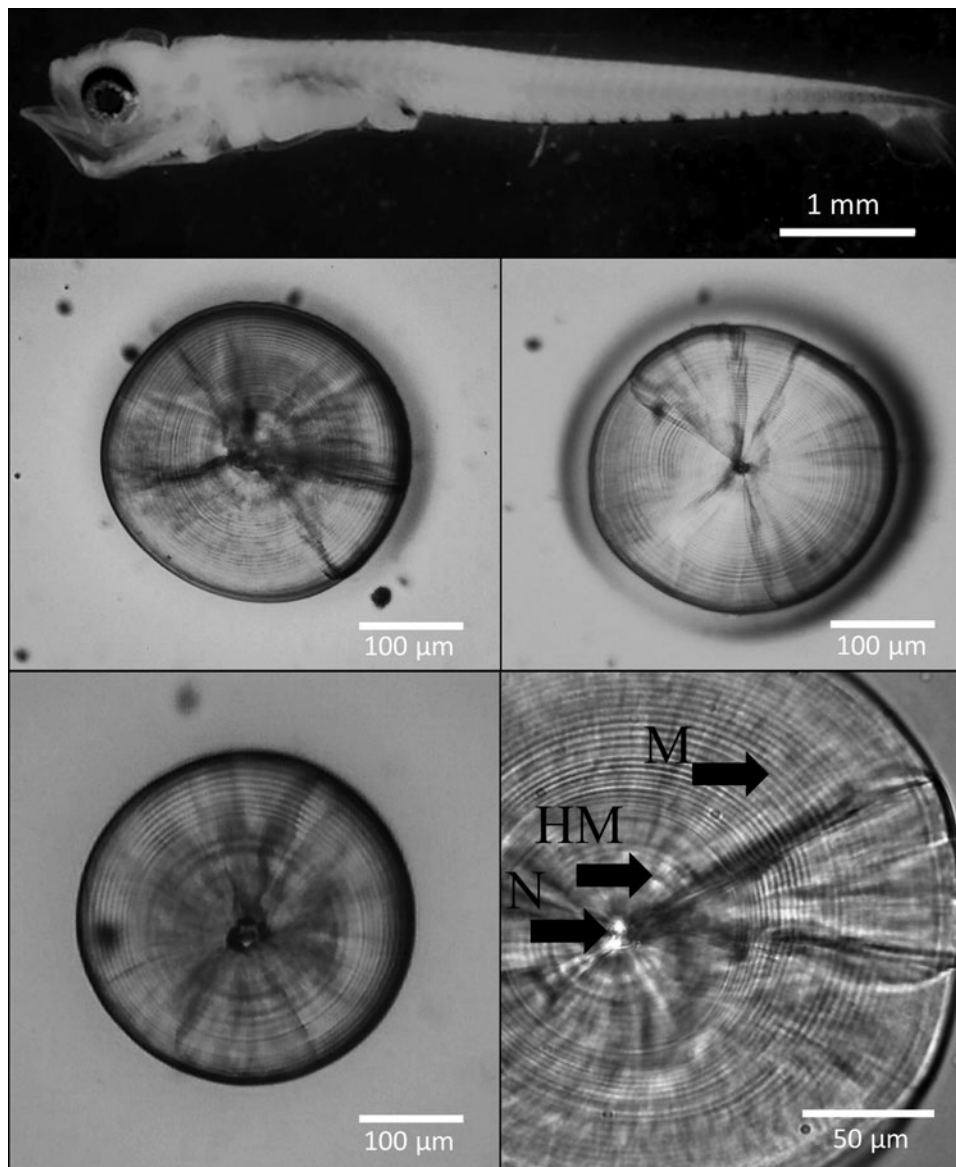


Fig. 2. Larva of the labrisomid blenny *Auchenionchus crinitus* (Jenyns, 1842), 5.5 mm SL, and sagittal otoliths of several specimens. N, nucleus; HM, hatch mark; M, microincrements. Notice the lack of damage on the edges of the sagittae due to fixation in buffered 5% formalin for 24 h.

Laboratory work

In the laboratory, all larval fish were separated, counted and identified into the lowest possible taxon. Labrisomid blenny larvae, *Auchenionchus crinitus*, were identified based on characteristic pigments, i.e. presence of a punctuated pigment in the base of the anus and a dendritic melanophore ventrally in the mid-tail, and genetically confirmed. Larval abundance was standardized to individuals (ind.) 100 m^{-3} using the flowmeter counts. The notochord length (NL), from the tip of the snout to the tip of the notochord in pre-flexion larvae or the standard length (SL), from base of the hypural bones in flexion and post-flexion larvae, was measured ($N = 486$) to the nearest 0.01 mm under an Olympus SZ-61 stereomicroscope with a Moticam 2500 (5.0 M pixel) video camera connected to a PC with the Moticam Image Plus 2.0 software. The larval measurements were not corrected for shrinkage.

Larval abundance per sampling day was compared using Kruskal–Wallis H test, because data departed from normality (Shapiro–Wilk test, $W = 0.81$, $P < 0.001$). Median and MAD (median absolute deviation) were used to describe basic statistics, when data departed from normality.

The left and right sagittal otoliths were removed from 405 well-preserved larvae (4.01 mm NL–12.50 mm SL; [Figure 2](#)). No previous grinding or polishing was necessary for the otolith reading. The otoliths were embedded in epoxy resin on a glass slide. The daily age was estimated by counting the number of otolith primary increments with a Motic BA310 light microscope at 1000 \times magnification under oil immersion.

Following Campana (1992), three independent counts were performed by the same reader (Valentina Nowajeswki, VN) on both the right and left sagittae ($N = 395$ pairs). Ages estimated using a subset of sagittae by the main reader (VN) and an experienced reader (Mauricio Landaeta) were not significantly different (Wilcoxon test, $P = 0.31$). Counts were performed after a prominent hatch mark (HM, [Figure 2](#)). The daily periodicity of microincrement deposition in *A. crinitus* has been previously validated by Mansur *et al.* (2013). Nonetheless, the first mark was not validated as a hatch mark. When the coefficient of variation (CV = standard deviation/mean $\times 100$) of the increment counts among the three readings was $< 10\%$, the mode of the three counts was calculated and utilized for the analysis. When the CV was $> 10\%$, the otolith reading was discarded ($N = 24$). Once selection

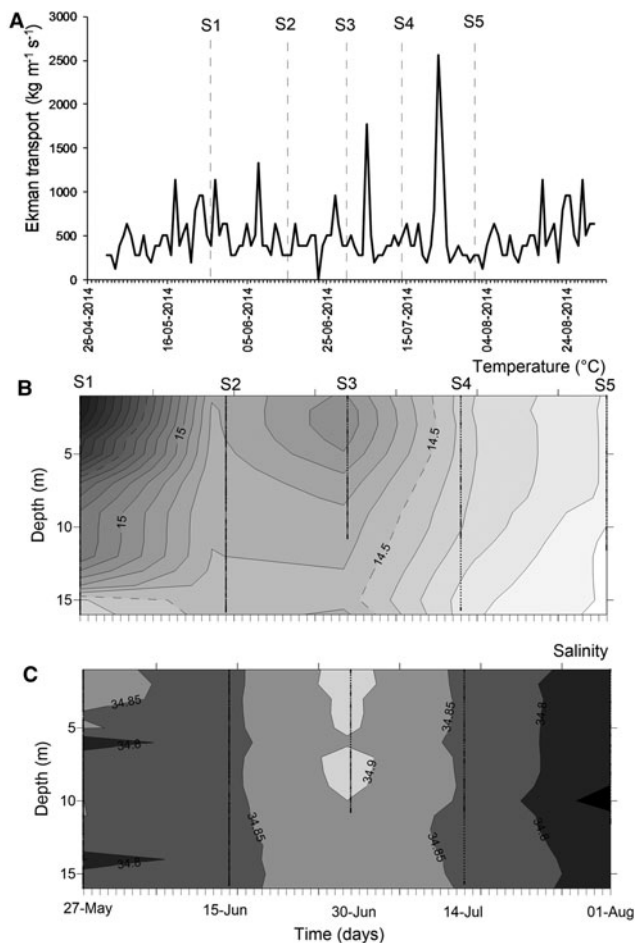


Fig. 3. Environmental conditions during the sampling period, austral autumn–winter 2014 off northern Chile. (A) Temporal series of wind-derived Ekman transport; (B) vertical section of water temperature ($^{\circ}\text{C}$); (C) vertical section of salinity. S1–S5 corresponds to the sampling dates.

of the values was done, comparison of readings was carried out with a Wilcoxon matched pairs test, testing the null hypothesis that reading of the left sagitta is the same as that of the right sagitta. Because the null hypothesis of the same result in both otoliths cannot be rejected ($W = 71.50$; $P = 0.51$), any of the otoliths can be utilized for analyses.

The hatch day composition of all aged larvae was subsequently estimated in a calendar year, and cohorts were identified according to the temporal pattern of hatching. Additionally, back-calculated hatching dates were related to the lunar cycle. For each sampling date, the days since new moon were counted (DNM), and thereby assigned DNM values for 0 to 29 for each date, in which 0 represented the new moon. The DNM values were converted to angles ($^{\circ}$) by dividing by 29 (the length, in days, of the lunar cycle) and then multiplying by 360° , so that the data could be analysed using circular statistics. To assess whether the hatching events showed lunar periodicity, the data were analysed with Rayleigh and Rao's spacing tests (Batschelet, 1981) using Past 3.11 software.

Least-squares simple linear regressions ($SL = a + bA + \varepsilon_i$) between the microincrement counts (age, A) and larval lengths (NL and SL) were adjusted, separately for each batch identified during autumn–winter 2014. In the model, the slope corresponded to the batch growth rate, and the intercept corresponded to the estimated hatch size. The comparison of the slopes of the regression models was carried out following Zar (2010).

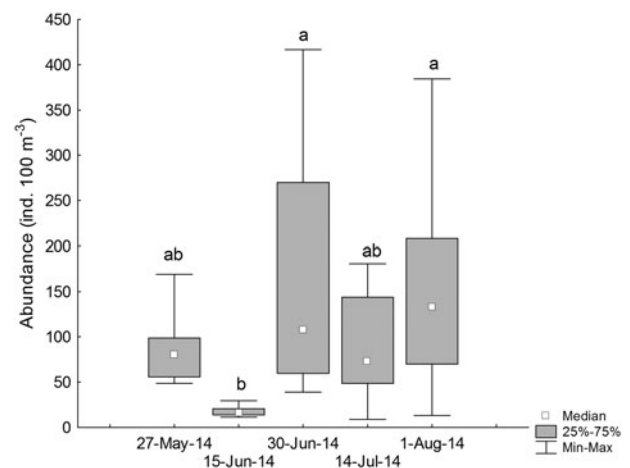


Fig. 4. Temporal variations in the standardized abundance (ind. 100 m^{-3}) of larval labrisomid blenny *Auchenionchus crinitus*. Different letters indicate significant differences ($P < 0.05$) among sampling dates.

Results

Physical settings

At mesoscale, several upwelling events were detected through the temporal series of wind-derived Ekman transport of autumn–winter 2014 (Figure 3A). Prior to the S1, there was ~ 10 days of winds favourable for upwelling events. After that, peaks of Ekman transport occurred only for few (<4) days, such as those occurring during 5 July ($1774.9\text{ kg m}^{-2}\text{ s}^{-1}$) and 23 July 2014 ($2555.9\text{ kg m}^{-2}\text{ s}^{-1}$) (Figure 3A). Moreover, the biological sampling did not match with large events of offshore transport.

During the sampling period, seawater temperature in shallow areas ranged between 13.97 and 16.32°C (mean \pm SD, $14.73 \pm 0.58^{\circ}\text{C}$). The warmest waters occurred during mid-May (Figure 3B), when the greatest vertical gradient was also detected (1.59 – 2.09°C). During the rest of the study, the water column was well-mixed, with temperature varying from 13.97 to 14.99°C ($14.43 \pm 0.27^{\circ}\text{C}$). Similarly, salinity was conservative, ranging between 34.65 – 34.95 (34.84 ± 0.04); an intrusion of relatively saltier waters was observed during late June 2014 (Figure 3C). Except for the first sampling day, no clear evidence of upwelling waters was detected in nearshore areas during autumn–winter 2014.

Larval abundance and size structure

During 27 May and 15 June 2014 (austral autumn), larval abundances were 39.06 ± 5.08 ind. 100 m^{-3} (median \pm MAD), with a significant increase during 30 June and 1 August 2014 (110.98 ± 47.66 ind. 100 m^{-3}) (Kruskal–Wallis test, $H_{4,40} = 16.32$, $P = 0.002$, Figure 4, Table 1).

Larval length varied between 4.01 and 12.50 mm SL ($N = 486$, median \pm MAD, 6.55 ± 1.13 mm SL) (Figure 5, Table 1). Size distribution did not follow a normal distribution (Shapiro–Wilk's test, $W = 0.97$; $P < 0.001$, Figure 5). The length distribution showed positive skewness and a leptokurtic distribution with a value greater than would be expected under the normal distribution on 15 June 2014 (Table 1); furthermore, the size distribution of collected larvae on other sampling days showed low skewness; some days had negative kurtosis values that would suggest an almost uniform distribution (Table 1).

Back-calculated hatch dates

The back-calculated hatch dates indicate the presence of three cohorts during the study period, two from autumn (cohort 1

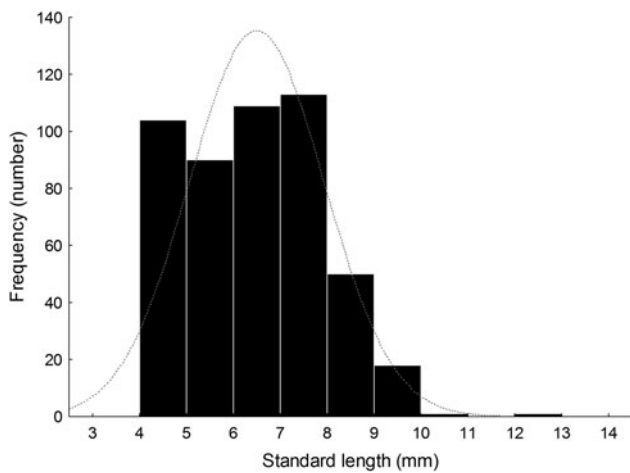


Fig. 5. Histogram of notochord or standard length (NL or SL, mm) of larval labrisomid blenny *Auchenionchus crinitus* collected during the whole studied period. Grey dotted line corresponds to the expected normal distribution.

from 6 May to 24 May; cohort 2 from 27 May to 19 June) and one from winter (cohort 3 from 20 June to 18 July) (Figure 6A). The first two main hatching events occurred during neap tides, and the third one was spread over most of the lunar cycle. Hatching was not homogeneous throughout the lunar cycle (Rayleigh test, $R=0.37$, $P<0.001$; Rao's spacing test, $U=330.4$, $P<0.001$) (Figure 6B), and centred during full moon (circular mean = day 13.09, 95% confidence interval: 12.02–14.18 day of the lunar cycle).

Size at hatch and larval age and growth by batch

For all three batches, the estimated age of larval *A. crinitus* varied between 3 and 30 days old. Estimated size at hatch varied from 3.23 ± 0.16 mm NL during May to 3.70 ± 0.35 mm NL during late July. Batch 1 experienced a mean growth rate of 0.22 ± 0.01 mm day⁻¹, while larvae hatched during early June (batch 2) and late July (batch 3) grew at 0.20 ± 0.01 mm day⁻¹ and 0.19 ± 0.02 mm day⁻¹, respectively (Figure 7). Estimated larval growth rates were similar among batches (homogeneity of slope test, $F=0.85$, $P=0.43$).

Discussion

Microstructure analysis of sagittal otoliths of larval labrisomid blenny *Auchenionchus crinitus* allows inferring the hatching of three batches during autumn–winter 2014 in nearshore waters off Isla Santa María, Antofagasta, northern Chile. Back-calculated hatch dates occurred throughout the lunar cycle, except during the new moon. This indicates that there is no timing periodicity with the moon, and it may be related to the adult timing of the reproductive events in labrisomid fish (Gibran *et al.*, 2004).

Larval *A. crinitus* increased in abundance from autumn to winter. During winter, a relatively large concentration of Chl-a in the inshore areas has been described (Morales *et al.*, 1996), supporting a large abundance of copepods (Hidalgo *et al.*, 2010), the main prey item of labrisomid larval fishes (Vera-Duarte & Landaeta, 2016).

Seawater hydrographic features were kept relatively similar during autumn and winter, as well as the estimated size-at-hatch and growth rates of larval *A. crinitus*. For cryptobenthic fish species, larval growth rates seem to vary at larger temporal scales, such as in stargazers (family Dactyloscopidae, Rodríguez-Valentino *et al.*, 2015; Castillo-Hidalgo *et al.*, 2018). The lack of seasonality

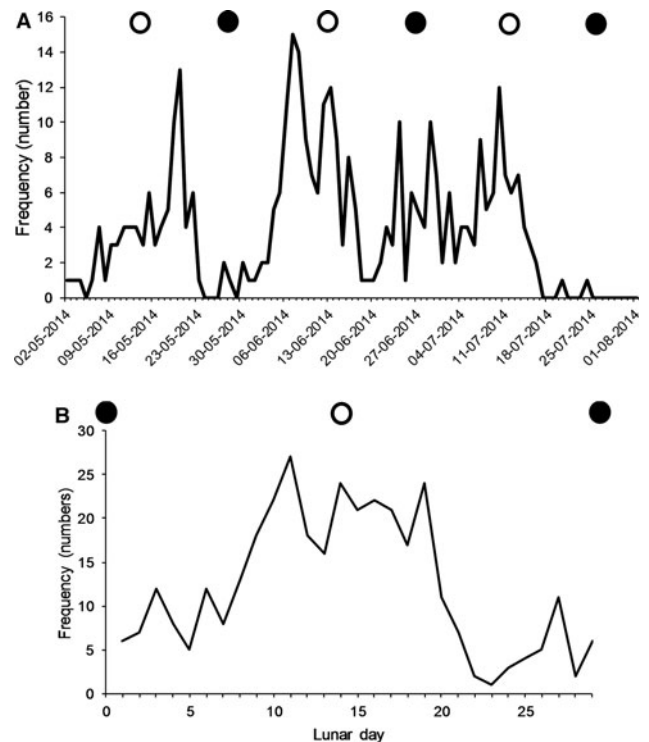


Fig. 6. Back-calculated hatch days of labrisomid blenny *Auchenionchus crinitus* during autumn–winter 2014 off northern Chile. (A) Hatch-days on an annual basis, (B) hatch-days on a lunar basis.

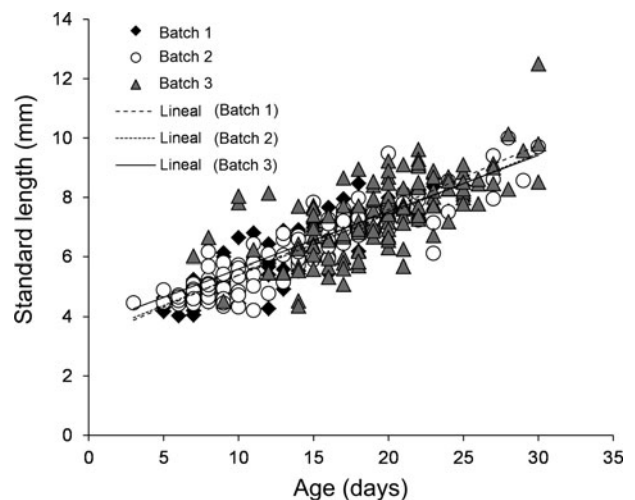


Fig. 7. Growth rate models for all three batches of larval *Auchenionchus crinitus* collected during the study period. Black diamonds, batch 1; white circles, batch 2; grey triangles, batch 3.

in the early life history traits of *A. crinitus* may be linked to the environmental stability of the water column structure.

Growth rates estimated for larval *A. crinitus* were similar to those described for other cryptobenthic fish larvae (clingfishes, Contreras *et al.*, 2013; triplefin, Palacios-Fuentes *et al.*, 2014; sand stargazer, Rodríguez-Valentino *et al.*, 2015) and adults (e.g. gobiids *Eviota* spp., 0.20 – 0.25 mm day⁻¹, Depczynski & Bellwood, 2006). Instead, mesopelagic larval species grew slower (0.05 – 0.06 mm day⁻¹) in shallow waters of northern Chile (Landaeta *et al.*, 2015), while epipelagic species, such as anchovy *Engraulis ringens*, grow faster (0.50 – 0.85 mm day⁻¹) during their early life stages in the same period (May–June, Contreras *et al.*, 2017). This suggests that growth patterns, which may be affected by oceanographic conditions, are species-specific in their

responses, considering pelagic vs benthic adults. In species with benthic adults, larval growth rates are remarkably similar, suggesting that the life history strategy explains changes in growth rate.

Larval *A. crinitus* collected with Bongo nets in the water column varied between 3 and 30 days old. According to otolith microstructure analysis of young-of-the-year collected in tidal pools, the pelagic larval duration (PLD) for the species is 73–75 days (Mansur et al., 2014). It is plausible that after the first month of life, postlarvae inhabit near-bottom, subtidal environments, entering next to the tide rock pools.

Acknowledgements. We appreciate the field and lab support of Dra. Gabriela Muñoz (Universidad de Valparaíso) and Dra. María T. González (Universidad de Antofagasta). Comments of two anonymous reviewers improved an early version of the manuscript.

Financial support. This research was partially funded by Comisión Nacional de Investigación Científica y Tecnológica (CONICYT) through projects Fondecyt 1120868 and Fondecyt 1150296.

References

- Batschelet E (1981) *Circular Statistics in Biology*. New York, NY: Academic Press.
- Bergenius MA, Meekan MG, Robertson RD and McCormick MI (2002) Larval growth predicts the recruitment success of a coral reef fish. *Oecologia* **131**, 521–525.
- Campana SE (1992) Measurement and interpretation of the microstructure of fish otoliths. In Stevenson DK and Campana SE (eds), *Otolith Microstructure and Analysis*, Vol. 117. Ottawa: Canadian Special Publication in Fisheries and Aquatic Sciences, pp. 59–71.
- Campana SE and Neilson JD (1985) Microstructure of fish otoliths. *Canadian Journal of Fisheries and Aquatic Sciences* **42**, 1014–1032.
- Carvalho MG, Moreira C, Queiroga H, Santos PT and Correia AT (2015) Ontogenetic development of the sagittal otoliths of *Lipophrys pholis* (Blenniidae) during the embryonic, larval and settlement stages. *Ichthyological Research* **62**, 351–356.
- Castillo-Hidalgo G, Plaza G, Diaz-Astudillo M and Landaeta MF (2018) Seasonal variations in the early life traits of *Sindoscopus australis* (Blennioidei: Dactyloscopidae): hatching patterns, larval growth and bilateral asymmetry of otoliths. *Journal of the Marine Biological Association of the United Kingdom* **98**, 1477–1485. doi: 10.1017/S0025315417000790.
- Chambers RC and Miller TJ (1995) Evaluating fish growth by means of otolith increment analysis: special properties of individual-level longitudinal data. In Secor DH, Dean JM and Campana E (eds), *Recent Developments in Otolith Research*. Columbia, SC: University of South Carolina Press, pp. 155–175.
- Contreras JE, Landaeta MF, Plaza G, Ojeda FP and Bustos CA (2013) The contrasting hatching patterns and larval growth of two sympatric clingfishes inferred by otolith microstructure analysis. *Marine and Freshwater Research* **64**, 157–167.
- Contreras JE, Rodríguez-Valentino C, Landaeta MF, Plaza G, Castillo MI and Alvarado-Niño M (2017) Growth and mortality of larval anchoveta *Engraulis ringens*, in northern Chile during winter and their relationship with coastal hydrographic conditions. *Fisheries Oceanography* **26**, 603–614.
- Depczynski M and Bellwood DR (2003) The role of cryptobenthic reef fishes in coral reef trophodynamics. *Marine Ecology Progress Series* **256**, 183–191.
- Depczynski M and Bellwood DR (2006) Extremes, plasticity, and invariance in vertebrate life history traits: insights from coral reef fishes. *Ecology* **87**, 3119–3127.
- Fontes J, Santos RS, Afonso P and Caselle JE (2011) Larval growth, size, stage duration and recruitment success of a temperate reef fish. *Journal of Sea Research* **65**, 1–7.
- Gibran FZ, Santos FB, dos Santos HF and Sabino J (2004) Courtship behavior and spawning of the hairy blenny *Labrisomus nuchipinnis* (Labrisomidae) in southeastern Brazil. *Neotropical Ichthyology* **2**, 163–166.
- Gibson RN (1970) Observations on the biology of the giant goby *Gobius cobitis* Pallas. *Journal of Fish Biology* **2**, 281–288.
- Hidalgo P, Escribano R, Vergara O, Jorquera E, Donoso K and Mendoza P (2010) Patterns of copepod diversity in the Chilean coastal upwelling system. *Deep Sea Research II* **57**, 2089–2097.
- Kohn YY and Clements KD (2011) Pelagic larval duration and population connectivity in New Zealand triplefin fishes (Tripterygiidae). *Environmental Biology of Fishes* **91**, 275–286.
- La Mesa M, Vera-Duarte J and Landaeta MF (2017) Early life history traits of *Harpagifer antarcticus* (Harpagiferidae, Notothenioidei) from the South Shetland Islands during austral summer. *Polar Biology* **40**, 1699–1705.
- Landaeta MF, López G, Suárez-Donoso N, Bustos CA and Balbontín F (2012) Larval fish distribution, growth and feeding in Patagonian fjords: potential effects of freshwater discharge. *Environmental Biology of Fishes* **93**, 73–87.
- Landaeta MF, Contreras JE, Bustos CA and Muñoz G (2015) Larval growth of two species of lanternfish at nearshore waters from an upwelling zone based on otolith microstructure analysis. *Journal of Applied Ichthyology* **31**, 106–113.
- Leis JM (1991) The pelagic stage of reef fishes. In Sale PF (ed.), *The Ecology of Fishes on Coral Reefs*. San Diego, CA: Academic Press, pp. 183–230.
- Mansur I, Catalán D, Plaza G, Landaeta MF and Ojeda FP (2013) Validations of the daily periodicity of increment deposition in rocky intertidal fish otoliths of the south-eastern Pacific Ocean. *Revista de Biología Marina y Oceanografía* **48**, 629–633.
- Mansur I, Plaza G, Landaeta MF and Ojeda FP (2014) Planktonic duration in fourteen species of intertidal rocky fishes from the south-eastern Pacific Ocean. *Marine and Freshwater Research* **65**, 901–909.
- Morales CE, Blanco JL, Braun M, Reyes H and Silva N (1996) Chlorophyll-*a* distribution and associated oceanographic conditions in the upwelling region off northern Chile during the winter and spring 1993. *Deep Sea Research I* **43**, 267–289.
- Muñoz AA and Ojeda FP (1997) Feeding guild structure of a rocky intertidal fish assemblage in central Chile. *Environmental Biology of Fishes* **49**, 471–479.
- Palacios-Fuentes P, Landaeta MF, Jahnsen-Guzmán N, Plaza G and Ojeda FP (2014) Hatching patterns and larval growth of a triplefin from central Chile inferred by otolith microstructure analysis. *Aquatic Ecology* **48**, 259–266.
- Panella G (1971) Fish otoliths: daily growth layers and periodical patterns. *Science* **173**, 1124–1127.
- Plaza G, Landaeta MF, Espinoza CV and Ojeda FP (2013) Daily growth patterns of six species of young-of-the-year of Chilean intertidal fishes. *Journal of the Marine Biological Association of the United Kingdom* **93**, 389–395.
- Pond S and Pickard GL (1983) *Introductory Dynamical Oceanography*, 2nd Edn. Oxford: Pergamon Press.
- Riginos C and Victor BC (2001) Larval spatial distributions and other early life-history characteristics predict genetic differentiation in eastern Pacific blennioid fishes. *Proceedings of the Royal Society of London B* **268**, 1931–1936.
- Robertson DR, Petersen CW and Brawn JD (1990) Lunar reproductive cycles of benthic-brooding reef fishes: reflections of larval biology or adult biology? *Ecological Monographs* **60**, 311–329.
- Rodríguez-Valentino C, Landaeta MF, Castillo-Hidalgo G, Bustos CA, Plaza G and Ojeda FP (2015) Interannual variations in the hatching pattern, larval growth and otolith size of a sand-dwelling fish from central Chile. *Helgolander Marine Research* **69**, 438.
- Sáez S and Pequeño G (2009) Updated, illustrated and annotated taxonomic key for fishes of the family Labrisomidae from Chile (Perciformes, Blennioidei). *Gayana* **73**, 130–140.
- Stenevik EK, Fossum P, Johannessen A and Folkvord A (1996) Identification of Norwegian spring spawning herring (*Clupea harengus* L.) larvae from spawning grounds off western Norway applying otolith microstructure analysis. *Sarsia* **80**, 285–292.
- Stephens Jr JS and Springer VG (1973) Clinid fishes of Chile and Peru, with description of a new species, *Myxodes ornatus*, from Chile. *Smithsonian Contributions to Science* **159**, 1–24.
- Uribe RA, Ortiz M, Macaya EC and Pacheco AS (2015) Successional patterns of hard-bottom microbenthic communities at kelps bed (*Lessonia trabeculata*) and barren ground sublittoral systems. *Journal of Experimental Marine Biology and Ecology* **472**, 180–188.
- Vera-Duarte J and Landaeta MF (2016) Diet of labrisomid blenny *Auchenionchus variolosus* (Valenciennes, 1836) (Labrisomidae) during its larval development off central Chile (2012–2013). *Journal of Applied Ichthyology* **32**, 46–54.
- Zar JH (2010) *Biostatistical Analysis*, 5th Edn. Englewood Cliffs, NJ: Prentice Hall.